

Bacteria-Based Materials for Stem Cell Engineering

Jake J. Hay, Aleixandre Rodrigo-Navarro, Michaela Petaroudi, Anton V. Bryksin, Andrés J. García, Thomas H. Barker, Matthew J. Dalby,* and Manuel Salmeron-Sanchez*

Materials can be engineered to deliver specific biological cues that control stem cell growth and differentiation. However, current materials are still limited for stem cell engineering as stem cells are regulated by a complex biological milieu that requires spatiotemporal control. Here a new approach of using materials that incorporate designed bacteria as units that can be engineered to control human mesenchymal stem cells (hMSCs), in a highly dynamic-temporal manner, is presented. Engineered *Lactococcus lactis* spontaneously colonizes a variety of material surfaces (e.g., polymers, metals, and ceramics) and is able to maintain growth and induce differentiation of hMSCs in 2D/3D surfaces and hydrogels. Controlled, dynamic, expression of fibronectin fragments supports stem cell growth, whereas inducible-temporal regulation of secreted bone morphogenetic protein-2 drives osteogenesis in an on-demand manner. This approach enables stem cell technologies using material systems that host symbiotic interactions between eukaryotic and prokaryotic cells.

Human mesenchymal stem cells (hMSCs) reside in niches, such as the bone marrow. These niches act to control hMSC quiescence, self-renewal, and differentiation upon regenerative demand.^[1] As hMSCs are anchorage dependent, they receive critical information through the extracellular matrix (ECM)

Dr. J. J. Hay, Dr. A. Rodrigo-Navarro, M. Petaroudi,
Prof. M. J. Dalby, Prof. M. Salmeron-Sanchez
Centre for the Cellular Microenvironment
University of Glasgow
Glasgow G12 8LT, UK
E-mail: Matthew.Dalby@glasgow.ac.uk;
Manuel.Salmeron-Sanchez@glasgow.ac.uk

Dr. A. V. Bryksin
Molecular Evolution Core Facility
Georgia Institute of Technology
950 Atlantic Dr NW, Atlanta GA 30332, USA

Prof. A. J. García
Woodruff School of Mechanical Engineering
Georgia Institute of Technology
315 Ferst Dr NW, Atlanta GA 30332, USA

Prof. T. H. Barker
Department of Cell Biology
University of Virginia
415 Lane Road, Charlottesville, Virginia VA 22904, USA

 The ORCID identification number(s) for the author(s) of this article can be found under <https://doi.org/10.1002/adma.201804310>.

© 2018 The Authors. Published by WILEY-VCH Verlag GmbH & Co. KGaA, Weinheim. This is an open access article under the terms of the Creative Commons Attribution License, which permits use, distribution and reproduction in any medium, provided the original work is properly cited.

DOI: 10.1002/adma.201804310

comprising the niche environment.^[2] The ECM is a complex and heterogeneous network of adhesive proteins and growth factors that support and guide cells.^[3] Recent studies using material interfaces have demonstrated that cell behaviors, such as differentiation, can be controlled through characteristics such as substrate stiffness,^[4] nanotopography,^[5] and chemistry.^[6] However, these are static systems and thus can only act as highly reductionist representations of in vivo ECM features.

There have been attempts to recapitulate the dynamic properties of the ECM using materials that react to external stimuli and ultimately alter the phenotype of the cells. Different types of triggering mechanisms have been utilized including light, either in 2D or 3D (hydrogels) culture systems, inducing irreversible or reversible protein-material interactions,^[7–10] temperature,^[11] and enzymes.^[12] However, these systems are typically designed to reveal or hide cell binding sites to/from cells and this still falls short of the dynamic nature of complex niches hMSCs reside in in vivo. There is still a need to develop approaches where both the physical properties and biological composition of the ECM can be dynamically controlled to recapitulate the properties of the hMSC native microenvironment.

Bacteria can be genetically modified to express different proteins which can be used to direct cell behavior and thus influence hMSC fate. Some authors have used bacterial secretion systems (e.g., Type III Secretion System (T3SS)) to directly inject transcription factors in eukaryotic cells.^[13] We propose that nonpathogenic bacteria, specifically the lactic bacteria *Lactococcus lactis*, can be utilized as a dynamic interface on materials to enable stem cell technologies. While use of materials containing bacteria appears counterintuitive in a system designed for eukaryotic cells, we show conditions for long term symbiosis of both cell populations within material systems. As well as being able to direct eukaryotic cell phenotype, bacteria interface with biomaterials of different physical properties enabling physical and biological control of hMSCs.

The control of hMSC fate is achieved functionalizing material system through engineered *L. lactis* that express the III_{7–10} fragment of the human fibronectin (FNIII_{7–10}) that is known to support cell adhesion^[14] and the bone morphogenetic protein 2 (BMP-2—membrane-bound and secreted), a cytokine pertaining to the transforming growth factor beta superfamily that can induce osteogenic differentiation in hMSCs.^[15] We showed that the differentiation of MSCs occur on engineered *L. lactis* that express FN if BMP-2 is added exogenously in the culture

medium.^[16] Here we demonstrate a step change by engineering materials containing bacteria that express proteins constitutively or triggered by an external stimulus. We show that these bacteria-based materials can be produced in 2D and 3D and offer new avenues to dynamic control of hMSCs.

Figure 1 illustrates a monolayer of engineered *L. lactis* that acts as an interface between synthetic materials and mammalian cells (Figure 1A). *L. lactis* have been genetically modified to express FNIII₇₋₁₀ that is covalently bound to the cell membrane to permit mammalian cell adhesion to the bacterial interface. Furthermore, BMP-2 is engineered so that it is either membrane bound, i.e., presented from the interface, or secreted to the extracellular medium (from hereon denoted *L. lactis*-BMP-2M [membrane] and *L. lactis*-BMP-2S [secreted]) to induce osteogenic

differentiation of hMSCs (Figure 1B). Importantly, these proteins can be synthesized in either a constitutive or inducible fashion, using the Nisin-controlled gene expression (NICE) system (nisA promoter), to provide dynamic-temporal control.^[17]

FNIII₇₋₁₀ contains the cell adhesion arginine-glycine-aspartic acid motif in the III₁₀ module and the adhesion-synergy proline-histidine-serine-arginine-asparagine (PHSRN) motif in the III₉ module. These two motifs interact with integrins, particularly $\alpha 5 \beta 1$.^[18] BMP-2 interacts with bone morphogenetic protein receptors (BMPRs) which leads to the activation of transcription factors that drive the transcription of genes related to osteogenic differentiation.^[19] Co-operation between integrin-driven adhesion and BMP-2 signaling has been shown to be potentially osteogenic.^[20]

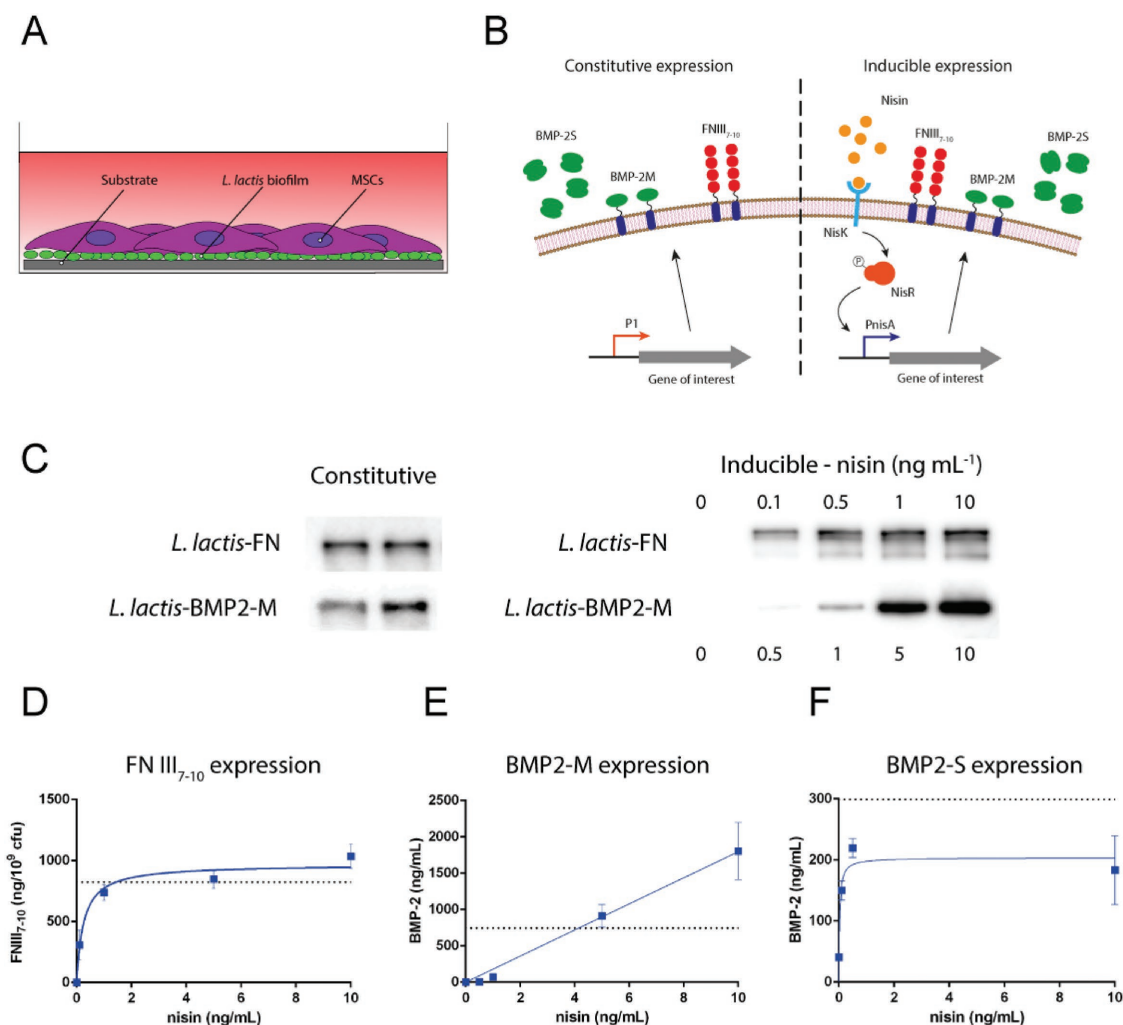


Figure 1. Overview of the system and protein expression analysis (*L. lactis* NZ9020). A) *L. lactis* biofilms spontaneously develop on top of the material substrate displaying and secreting a variety of proteins and acting as an interface for hMSC attachment, proliferation, and differentiation. B) *L. lactis* engineered to express the III₇₋₁₀ fragment of the human fibronectin (FNIII₇₋₁₀) on its cell wall, fused to green fluorescent protein (GFP) as a reporter to initiate mammalian cell attachment. *L. lactis* can also be engineered to express BMP-2 as a membrane (BMP-2M) or secreted (BMP-2S) protein in a constitutive (left) or inducible (right) manner. BMP-2 signaling in mammalian cells leads to the activation of osteogenic transcription factors resulting in mesenchymal stem cell differentiation into osteoblasts. C) FN and BMP-2M were quantified via Western blot for both constitutive (left) and inducible (right) strains. Secreted BMP-2 was quantified by ELISA. Fresh GM17 growth media were inoculated with 20% overnight stationary phase culture and cultured for 1 h before the addition of nisin. Protein expression was measured after 5 h. Protein standards were used to construct a standard curve and concentrations were calculated from the regression analysis. These were quantified and plotted in ng mL⁻¹ against nisin induction for: D) FN, E) BMP-2M, and F) BMP-2S. The dotted lines represent protein expression values in the constitutive strains.

To confirm the expression of proteins by these interfaces, plasmids carrying the human FNIII_{7–10}^[21] and BMP-2 genes transformed to *L. lactis* strains were sequenced (data available in the Supporting Information) and protein expression was characterized using Western blot, enzyme-linked immunosorbent assay (ELISA), or fluorometry (Figure 1C and Figure S1, Supporting Information). Samples from the constitutive strains (Figure 1C—constitutive) show the presence of FNIII_{7–10} (*L. lactis*-FN), BMP-2M (*L. lactis*-BMP-2M) in the cell lysate, and BMP-2S (*L. lactis*-BMP-2S) in the supernatant (Figure S1D, Supporting Information). Furthermore, and more importantly, the dynamic expression of these proteins in response to different concentrations of nisin is demonstrated in Figure 1C—inducible. Protein expression is dependent on the concentration of the inducer (nisin) (Figure 1D–F). These results confirm the functionality of the cell environment by either membrane-bound or secreted proteins. Figure S1H in the Supporting Information shows the absolute protein expression values. We note that the amount of expressed protein is highly dependent on the strength of the promoter driving the expression. Notably, the *nisA* promoter induced with saturating amounts of nisin produces higher expression levels compared to the constitutive P1 promoter.^[22]

We assessed the use of two *L. lactis* strains, NZ9000 and NZ9020 at the cell/material interface. Both are derivatives of *L. lactis* MG1363,^[23] with the *nisRK* nisin sensing genes integrated in the *pepN* locus (genotype *pepN::nisRK*). This allows for the expression of the *nisK* sensor histidine kinase and *nisR* response regulator, required for nisin-induced gene expression^[24] (Figure 1B). *L. lactis* NZ9020^[23] lacks the *ldhA* and *ldhB* genes for lactate dehydrogenase, the last enzyme in the glycolytic pathway that metabolizes pyruvate to lactic acid.^[25] Accumulation of lactic acid leads to medium acidification, which adversely affects the viability of the hMSCs. Without lactate dehydrogenase, *L. lactis* shifts its homofermentative glycolysis metabolism toward the production of acetoin as the main by-product with trace amounts of ethanol and other metabolites^[23] (Figure S2E, Supporting Information). In the presence of oxygen, *L. lactis* switches its metabolism to aerobic respiration, using endogenous nicotinamide adenine dinucleotide oxidase to maintain its redox balance. By supplementing hemin in the growth medium at low concentrations, 5 $\mu\text{g mL}^{-1}$, the oxidation of NADH shifts to the electron transport chain^[26] and the production of lactic acid is significantly reduced.

Prior to coculturing hMSCs and *L. lactis*, we investigated the viability of *L. lactis* biofilms on materials for 28 d, the time frame required to complete osteogenic differentiation in hMSCs.^[27] As shown in a previous work,^[28] the biofilms developed on glass are stable up to 4 d, whilst biofilms developed on a more hydrophobic surface as poly(ethyl acrylate) (PEA) are stable up to 28 d, the maximum time frame required for hMSCs to commit and differentiate to the osteogenic lineage. To reduce bacterial proliferation, sulfamethoxazole (SMX) was thus used at 5 $\mu\text{g mL}^{-1}$ for the duration of the culture (Figure S2A,B, Supporting Information). Sulfamethoxazole is a bacteriostatic that blocks folate synthesis in bacteria, leading to a reduction in bacterial proliferation. Although the life cycle of a biofilm is limited, we found bacteria adhered to material substrates throughout the 28 d culture, with bacterial viability close to 70% (Figure S2A,B, Supporting Information).

Determination of biofilm density on the surfaces used in this work, glass and PEA, was performed elsewhere^[29] with values between 5×10^4 and 7.5×10^4 cfu mm^{-2} , that correspond to a coverage of ≈ 9 –14%. *L. lactis* produces biofilms that are usually one cell thick and do not fully cover the underlying substrate, as assessed by scanning electron microscopy on the surfaces tested in this work, namely glass, poly(ethyl acrylate), polycaprolactone (PCL), polyether ether ketone (PEEK), and titanium (Figure S4, Supporting Information). On the other hand, species such as *Staphylococcus aureus* and *Escherichia coli*, amongst others, produce thicker biofilms with an evident presence of secreted matrix components. The presence of these extracellular matrix components is less evident, if not totally absent, in the biofilms produced by *L. lactis*.

Next, hMSCs were cultured on *L. lactis* NZ9000 and NZ9020 biofilms expressing BMP-2M and BMP-2S, with *L. lactis*-FN, *L. lactis*-empty and FN-coated substrate as controls (FN-coated substrate and *L. lactis*-BMP-2S shown in Figure S3A, Supporting Information). After 28 d, hMSC viability values were higher than 95% for *L. lactis* NZ9020 (Figure 2B and Figure S2C, Supporting Information) and less than 40% for *L. lactis* NZ9000 (Figure S2D, Supporting Information) for all tested conditions, presumably due to the accumulation of lactic acid in the culture medium. The pH of the culture media of *L. lactis* NZ9020 and NZ9000, with and without hemin, was measured after 1 d of growth in both aerobic and anaerobic conditions (Figure S3B, Supporting Information). NZ9020 grown aerobically with hemin produced the closest to neutral pH value (7.1). Based on these results, it was decided to use *L. lactis* NZ9020 for the hMSCs differentiation experiments. The dotted line represents pH 7.4, the closest growth conditions to that of biological pH was reached by aerobic NZ9020 with hemin at 5 $\mu\text{g mL}^{-1}$.

We showed the ability of *L. lactis* to colonize a variety of different biomedical materials including polished titanium, PCL, and PEEK in 2D and 3D. Figure S4 in the Supporting Information shows that bacteria were able to form cfu biofilms with a heterogeneous structure and a thickness of one cell on all substrates, as assessed using scanning electron microscopy imaging.

hMSC adhesion to constitutive and inducible *L. lactis*-FN was tested after 5 h using increasing amounts of nisin (0, 0.5, 1, and 10 ng mL^{-1}). This led to increasing amounts of FNIII_{7–10} in the bacterial membrane as seen in Figure 1C,D and Figure S1A,B in the Supporting Information. In the interfaces with constitutive FN expression, the presence of the FNIII_{7–10} fragment induced hMSC adhesion and focal adhesion development on at the bacteria/material interface, similar to the FN-coated substrate, with cell areas of 2438 ± 245 and $3126 \pm 165 \mu\text{m}^2$, respectively (Figure 2A).^[29] Importantly, the FN protein expression system controlled by nisin shows that hMSC area increased with increasing nisin concentration (FN values for both inducible and constitutive expression in Figure 2A and Figure S5A in the Supporting Information are deduced from Western blot readings from Figure 1C and Figure S1A,B, Supporting Information) with average cell areas of $1308 \pm 120 \mu\text{m}^2$ without nisin induction and $2178 \pm 129 \mu\text{m}^2$ inducing with 10 ng mL^{-1} of nisin (Figure 2C).^[29] Importantly, the nisin-controlled FN protein expression system shows that hMSC area increased with

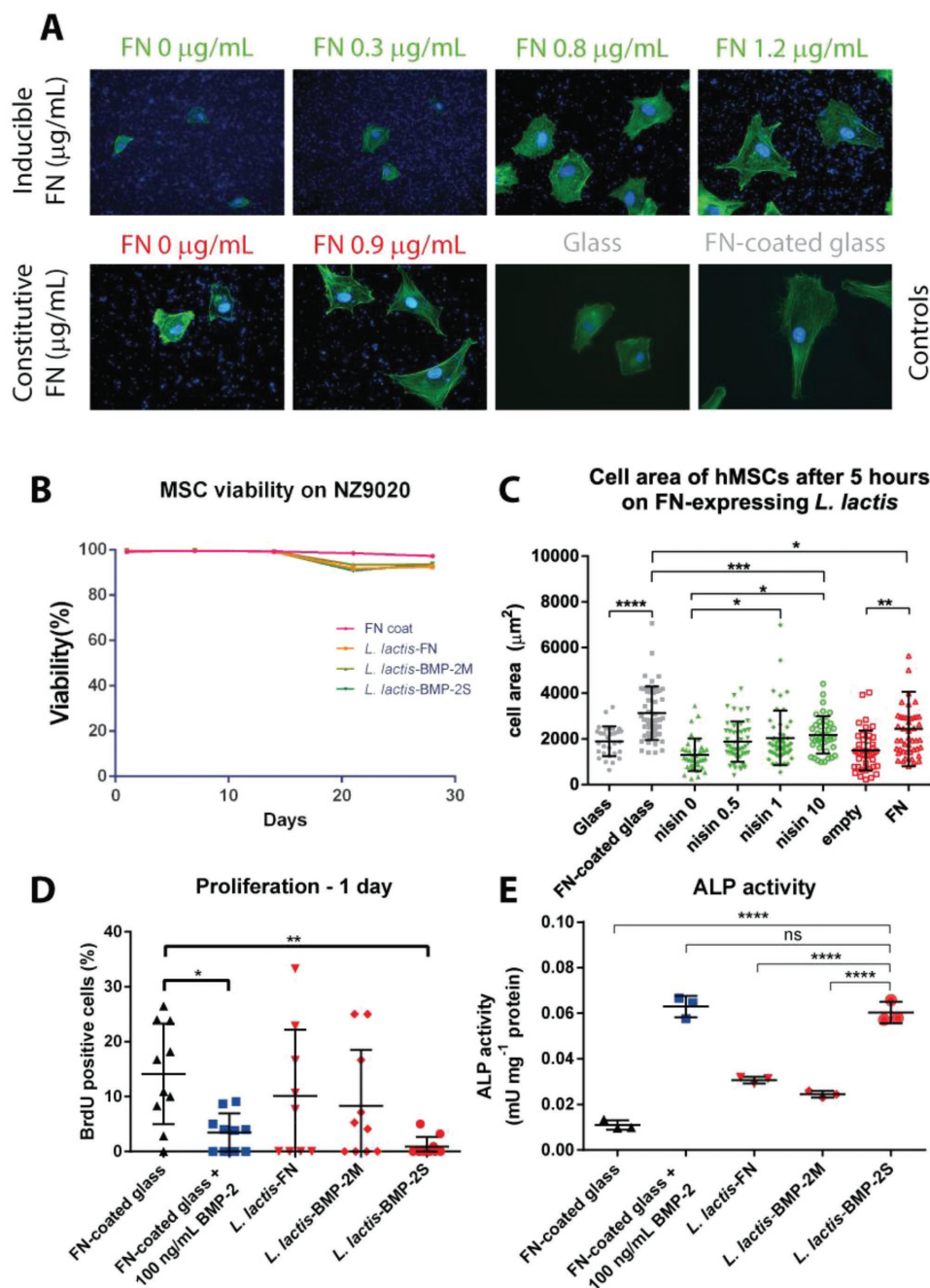


Figure 2. hMSC adhesion on *L. lactis* with inducible expression of FNIII₇₋₁₀. A) hMSCs were cultured over different FNIII₇₋₁₀-expressing strains of *L. lactis* for 5 h. Top row shows cells attached to inducibly expressed FNIII₇₋₁₀ under different concentrations of nisin. Bottom row shows hMSCs attached to constitutive expressing FN strains. FN-coated surfaces and glass were used as a positive and negative control respectively. hMSCs appear larger on samples where more FN is present. Scale bar is 100 μm . B) MSC viability on several *L. lactis* NZ9020 strains over 4 weeks. hMSC viability is roughly equivalent to that of an FN-coated substrate. C) Cell area of hMSCs was quantified from images in (A). Cell area increases upon additive amounts of nisin as more FN will be available to the hMSCs. The constitutive FNIII₇₋₁₀ and FN-coated substrate also show much higher cell area than their empty and glass counterparts. Data were shown to be normally distributed and is presented as mean \pm standard deviation (SD) and analyzed with analysis of variance (ANOVA) with a Tukey post hoc test. Significance levels are * $p < 0.05$, ** $p < 0.01$, and *** $p < 0.001$ (symbols represent individual data points). D) Cell proliferation on all surfaces after 1 d. The data are not normally distributed and were therefore analyzed with a nonparametric ANOVA with a Bonferroni post hoc test (symbols represent individual data points). E) Alkaline phosphatase expression in hMSCs after a 12 d culture. Graph shows that the cells cocultured with *L. lactis* NZ9020 BMP-2-S, which secretes $\approx 300 \text{ ng mL}^{-1}$ of BMP-2 in the culture medium, show a comparable amount of ALP expression when compared to the control culture, which is an FN-coated surface with medium supplemented with 100 ng mL^{-1} of recombinant human BMP-2. The rest of the cultures, FN-coated glass, *L. lactis*-FN, and *L. lactis*-BMP-2-M showed similar and statistically significantly lower values ALP activity values. These data suggest that the BMP-2 secreted by *L. lactis*, and only when secreted, is biologically active and induces the expression of alkaline phosphatase in hMSC. Data are presented as mean \pm SD and was analyzed with a parametric ANOVA with a Tukey post hoc test. Significance levels are * $p < 0.05$, ** $p < 0.01$, and *** $p < 0.001$ (symbols represent individual data points).

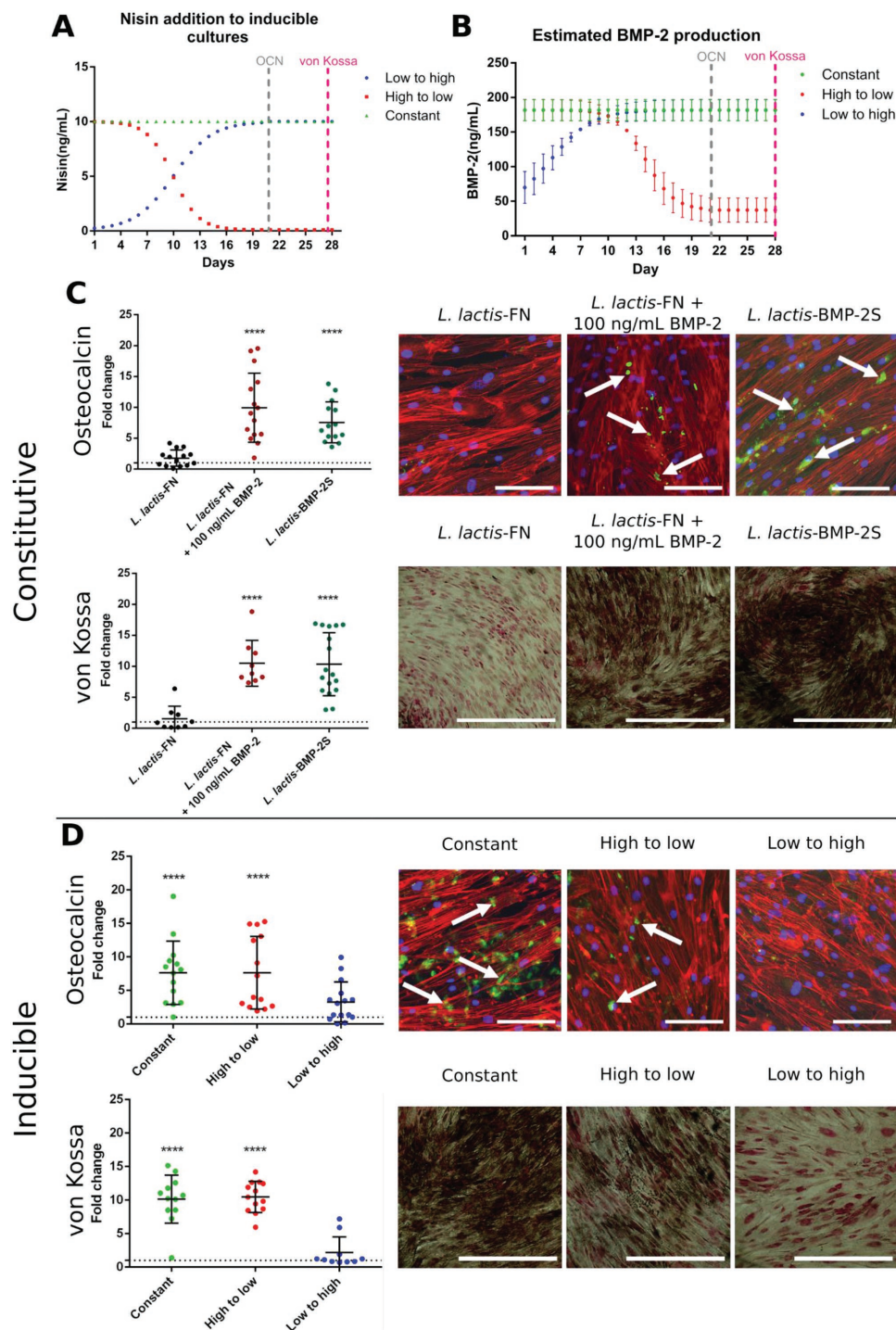


Figure 3. Osteogenic differentiation of hMSCs on *L. lactis* (NZ9020) with inducible expression of BMP-2. A) The inducible cultures were tailored to express BMP-2 at different rates and FN in a constant fashion throughout the course of the experiment to test the longevity and time dependency of BMP-2 toward osteogenic differentiation. We used a biofilm prepared by mixing two different strains in a 1:1 ratio; one strain produces FN constitutively, and the other secretes BMP-2 (*L. lactis* NZ9020 BMP-2S) in an inducible manner. Nisin was added daily to the cultures. A scatter plot of constant (green), high to low (red), and low to high (blue) induction profiles were chosen to test BMP-2S osteogenic activity. More information on the equation governing the induction profiles and the numerical values can be found in Table S1 in the Supporting Information. B) Levels of inducer (A) were related to absolute protein secretion as interpolated from (A). hMSCs were cultured on C) constitutive and D) inducible expressing bacteria for 21 d (OCN) and 28 d (von Kossa). At 21 d, hMSCs were stained for actin (red), osteocalcin (green), and nuclei (blue) and OCN was quantified. At 28 d hMSC mineralization was studied. Black deposits corresponding to calcium phosphate deposition were imaged and quantified. Total integrated density corresponding to the green channel (osteocalcin) and black channel (phosphate) were quantified. Controls can be found in the Supporting Information. Top images show OCN and phosphate deposition as a fold change increase against FN-coated substrate (arbitrary value of 1, represented

increasing nisin concentration (FN values for both inducible and constitutive expression in Figure 2A and Figure S5A in the Supporting Information are deduced from Western blot readings from Figure 1C and Figure S1A,B, Supporting Information) with average cell areas of $1308 \pm 120 \mu\text{m}^2$ without nisin induction and $2178 \pm 129 \mu\text{m}^2$ inducing with 10 ng mL^{-1} of nisin (Figure 2C).

hMSCs were cocultured on materials containing different *L. lactis* strains (constitutive FNIII₇₋₁₀, BMP-2M and BMP-2S) and proliferating cells were measured using 5-bromo-2'-deoxyuridine (BrdU) after 1 d coculture (Figure 2D). hMSCs on FN-coated substrates, *L. lactis*-FN and *L. lactis*-BMP-2M show high proliferation rates ($\approx 10\%$ of total cell count being BrdU positive). Conversely, lowest cell proliferation was seen on the FN-coated substrate samples cultured with BMP-2 control (100 ng mL^{-1} exogenous) of and *L. lactis*-BMP-2S, with less than 5% of cells being BrdU positive. No effect was found by fusing green fluorescent protein (GFP) to the expressed proteins (GFP was used to assay protein concentration, Figure S6, Supporting Information); a similar trend was seen in a 3 d proliferation experiment (Figure S6B, Supporting Information). These results indicate that hMSCs on materials containing *L. lactis*-BMP-2S are behaving in a similar manner to hMSCs on an FN-coated substrate cultured with media supplemented with 100 ng mL^{-1} BMP-2 and is in line with growth slow down with differentiation onset.^[27,30]

hMSC differentiation was investigated at different time points; at 12 d by alkaline phosphatase (ALP) activity, at 21 d by osteocalcin (OCN) expression, and at 28 d by matrix mineralization assessment (von Kossa staining). ALP catalyzes the hydrolysis of phosphate esters and plays a key role in osteoblast activity and skeletal mineralization.^[31] While *L. lactis*-FN and *L. lactis*-BMP-2M produced slightly increased levels of ALP compared to the control, *L. lactis*-BMP-2S produced significantly higher levels, equivalent to the 100 ng mL^{-1} exogenous BMP-2 positive control (Figure 2E, GFP clones shown in Figure S7, Supporting Information). For the longer term experiments (Figure 3), different time-dependent induction profiles were set up to test the effectiveness of different concentrations of bacterially secreted BMP-2, as this is one of the key features of this material interface, i.e., the ability to control the temporal profile of expression of proteins that trigger hMSC differentiation. Thus, constant (green), high-to-low (red), and low-to-high (blue) BMP-2 expression profiles were tested as shown in Figure 3A and Table S1 in the Supporting Information. Figure 3B shows the amount of BMP-2 expressed by *L. lactis*-BMP-2S after addition of nisin interpolated from the ELISA values shown in Figure 1F. We note that this is the amount of BMP-2 secreted in the standard conditions measured in Figure 1—the characterization of our raw material—and that the exact amount of BMP-2 secreted by bacteria in

coculture with hMSCs might be slightly different, influenced by the conditions of the media.

OCN is regularly used as a marker for the onset of osteogenic commitment as it is expressed postproliferatively by osteoblasts.^[32] Quantification of OCN (Figure 3C) showed higher expression in the 100 ng mL^{-1} BMP-2 positive control and in our constitutive *L. lactis*-BMP-2S interfaces. Deposition of phosphate, a marker of matrix mineralization denoting terminal osteoblast differentiation was measured at day 28 using von Kossa staining (Figure 3C). Image analysis reveals similar levels of mineralization between *L. lactis*-BMP-2S and the 100 ng mL^{-1} BMP-2, in good agreement with trends in proliferation, ALP, and OCN.

The dynamic character of the bacteria-based interface was used to investigate the temporal profile of BMP-2 delivery in relation to hMSC differentiation. Figure 3D shows hMSC differentiation in response to our inducible strains by both OCN and von Kossa staining. The profiles shown in Figure 3B were used to highlight these dynamics. The data show that BMP-2 is most effective during early culture, as results for constant and high-to-low BMP-2 delivery lead to the same level of osteogenic differentiation. In contrast, expressing the same amount of BMP-2 in the later stages of the culture (low-to-high, Figure 3B) have no effect in triggering hMSC differentiation within this time course. This is in agreement with other studies that indicate BMP-2 signaling to be a very early stage osteogenic trigger.^[30] Note that further OCN and von Kossa images are shown in Figures S8 and S9 in the Supporting Information, respectively. Together, all of these results demonstrate the potential of *L. lactis*-BMP-2S functionalized materials to promote hMSC differentiation.

L. lactis strains constitutively expressing BMP-2S driven by the P1 promoter were included in collagen sponges together with hMSCs to investigate adhesion and differentiation in 3D environments. Figure S10A in the Supporting Information shows that cells have attached to scaffolds functionalized with *L. lactis* biofilms prepared from early log-phase cultures, which reach a final bacterial concentration of $2.23 \times 10^9 \text{ cfu mL}^{-1}$ in GM17, with much higher cell count than collagen only systems. hMSC differentiation was quantified by ALP activity at day 15. Figure S10B in the Supporting Information shows that hMSCs in collagen sponges loaded with *L. lactis*-BMP-2S showed significantly increased osteogenic differentiation compared to collagen only and the other bacterial strains in agreement with 2D data.

L. lactis is a gram-positive lactic acid bacterium that has been used for centuries in food fermentation. Within the last 35 years, significant progress has been made in using this organism, amongst other bacterial species in genetic engineering for the therapeutic delivery of proteins.^[33-38] For example, interleukin 27 has been expressed to alleviate the symptoms of colitis in mice.^[39] Our work paves the way for

by the horizontal dotted line on the graphs) on constitutively expressed *L. lactis*-BMP-2S. Bottom images show OCN and phosphate deposition as a fold change increase against FN-coated substrate on inducibly expressed *L. lactis*-BMP-2S under the three induction profiles shown. Graphs show OCN and phosphate with standard deviation of the sample sets, $N \geq 400$ cells were analyzed for each condition. Data were shown to be normally distributed and is presented as mean \pm SD. Data were analyzed using an ANOVA with a Tukey post hoc test. Scale bar is $100 \mu\text{m}$ in OCN images and $300 \mu\text{m}$ in von Kossa images. The dotted lines in graphs in (C) and (D) correspond to the value of the fold change for the negative control (FN-coated surface). Significance levels are $*** p < 0.0001$ (symbols represent individual data points).

bacteria-based materials that enable hMSCs to be used in cell therapies. Current stem cell culture systems fall far short of desired outcomes of enhanced growth and enhanced proliferation that can work in a bioreactor-like manner.^[40] Furthermore, these culture systems are not dynamic and might be good for growth^[41] or differentiation^[4,5] but not for both. Dynamic culture systems have been developed but are limited typically to simple on/off states.^[6,11] Here we show how nonpathogenic bacteria such as *L. lactis* can be engineered and incorporated into material systems to allow temporal expression of membrane bound or secreted biologicals that can control hMSC growth (using FN) and differentiation (using BMP-2). It is easy to see how the complexity of this system can be tuned to express other proteins that could, e.g., drive other phenotypes. Further, the system is compatible with 3D materials, adherent stem cell cultures, such as hMSCs, can be scaled to 3D “fermentation” type bioreactors for mass production of cells.

We focus on BMP-2 and osteogenic hMSC as a proof of concept. Bone is the second most transplanted tissue after blood^[42] and thus, there is a growing need for lab grown osteoblasts for cellular therapies. The ageing populations of many countries only exacerbates the problem as diseases such as osteoporosis are becoming more prevalent.^[43] This work shows the osteogenic capabilities of genetically engineered bacteria in both 2D and 3D and on a variety of different materials (glass, polymers, hydrogels, and metal). We can coat these surfaces with BMP-2 secreting *L. lactis* to induce highly efficient differentiation of hMSCs to osteoblasts in vitro, with 3D systems allowing us to envisage bioreactor scale cell production. These cells can then be harvested for a variety of downstream applications, ranging from autologous or allogenic cell transplants or for the creation of lab grown bone.^[44]

Using these simple biological cells, the system could be improved as we created an environment whereby BMP-2 compounded with other growth factors would assist in the creation of a bacterially expressed osteogenic “cocktail”. BMP-7, platelet-derived growth factor, and fibroblast growth factor are all known osteogenic factors that in addition to BMP-2 could be engineered into *L. lactis* to provide temporal controlled release and hence more efficient differentiation of hMSCs in a manner that would be extremely different to using conventional biomaterials approaches. It is exactly this flexibility that is the real benefit concept. There are already a wide variety of constitutive and inducible expression systems available for *L. lactis*^[45–47] and with these tools, one can create a plethora of on–off controlled material systems to deliver the protein of interest at a desired time point and dose. This would allow the creation of highly dynamic materials with a wide range of temporal information delivered to stem cells.

Here, we demonstrate the potential for use of bacteria-based material systems to control multiple facets of hMSC behavior. Even if responsive materials for cell engineering have been already developed and tested, radically, we use a broad range of materials (synthetic and natural substrates, in 2D and 3D culture systems) that are functionalized with genetically engineered bacteria to form bacteria-based materials. The nonpathogenic bacteria *L. lactis* has been modified to express a fragment of human FN as a membrane bound protein, to enable mammalian cell adhesion. In addition, the system

has been further modified to express BMP-2, in a membrane bound and secreted form, under external induction. Whilst the membrane bound BMP-2 exhibited no osteogenic effect, secreted BMP-2 showed high levels of biological activity, being comparable to that of 100 ng mL⁻¹ of BMP-2. Short, mid and long-term tests all showed the biological activity of *L. lactis* secreting BMP-2, creating a new paradigm in hMSC engineering. These new materials can be instructed to produce biomolecules under demand, triggered by external stimuli. We foresee developments of this concept to produce large amounts of hMSCs in vitro and even adapting the system to be used in vivo in tissue engineering applications.

Supporting Information

Supporting Information is available from the Wiley Online Library or from the author.

Acknowledgements

J.J.H. and A.R.-N. contributed equally to this work. The support from the European Research Council (ERC306990), the UK Engineering and Physical Sciences Research Council (EP/P001114/1), and the Leverhulme Trust (RPG-2015-191) is acknowledged. M.J.D. and M.S.-S. designed the concept. A.R.-N., A.V.B., A.J.G., T.H.B., M.J.D., and M.S.-S. designed the experiments. J.J.H., A.R.-N., and M.P. performed the experiments. J.J.H. and A.R.-N. prepared figures. J.J.H., A.R.-N., A.J.G., T.H.B., M.J.D., and M.S.-S. wrote the paper. The hMSCs used were purchased from PromoCell.

Conflict of Interest

The authors declare no conflict of interest.

Keywords

cell engineering, dynamic materials, living materials, stem cells, synthetic biology

Received: July 7, 2018

Revised: August 11, 2018

Published online: September 12, 2018

- [1] F. M. Watt, B. L. M. Hogan, *Science* **2000**, 287, 1427.
- [2] M. Lutolf, P. Gilbert, H. Blau, *Nature* **2009**, 462, 433.
- [3] M. Aumailley, B. Gayraud, *J. Mol. Med.* **1998**, 76, 253.
- [4] A. J. Engler, S. Sen, H. L. Sweeney, D. E. Discher, *Cell* **2006**, 126, 677.
- [5] M. J. Dalby, N. Gadegaard, R. Tare, A. Andar, M. O. Riehle, P. Herzyk, C. D. Wilkinson, R. O. Oreffo, *Nat. Mater.* **2007**, 6, 407.
- [6] M. Ebara, M. Yamato, T. Aoyagi, A. Kikuchi, K. Sakai, T. Okano, *Biomacromolecules* **2004**, 5, 505.
- [7] S. Weis, T. T. Lee, A. del Campo, A. J. García, *Acta Biomater.* **2013**, 9, 8059.
- [8] J. C. Grim, T. E. Brown, B. A. Aguado, D. A. Chapnick, A. L. Viert, X. Liu, K. S. Anseth, *ACS Cent. Sci.* **2018**, 4, 909.
- [9] C. A. Deforest, D. A. Tirrell, *Nat. Mater.* **2015**, 14, 523.
- [10] K. A. Mosiewicz, L. Kolb, A. J. Van Der Vlies, M. M. Martino, P. S. Lienemann, J. A. Hubbell, M. Ehrbar, M. P. Lutolf, *Nat. Mater.* **2013**, 12, 1072.

- [11] S. J. Todd, D. J. Scurr, J. E. Gough, M. R. Alexander, R. V. Ulijn, *Langmuir* **2009**, *25*, 7533.
- [12] J. N. Roberts, J. K. Sahoo, L. E. McNamara, K. V. Burgess, J. Yang, E. V. Alakpa, H. J. Anderson, J. Hay, L. A. Turner, S. J. Yarwood, M. Zelzer, R. O. C. Oreffo, R. V. Ulijn, M. J. Dalby, *ACS Nano* **2016**, *10*, 6667.
- [13] F. Bai, Z. Li, A. Umezawa, N. Terada, S. Jin, *Biotechnol. Adv.* **2018**, *36*, 482.
- [14] M. M. Martino, M. Mochizuki, D. A. Rothenfluh, S. A. Rempel, J. A. Hubbell, T. H. Barker, *Biomaterials* **2009**, *30*, 1089.
- [15] A. C. Carreira, G. G. Alves, W. F. Zambuzzi, M. C. Sogayar, J. M. Granjeiro, *Arch. Biochem. Biophys.* **2014**, *561*, 64.
- [16] J. J. Hay, A. Rodrigo-Navarro, K. Hassi, V. Moulisova, M. J. Dalby, M. Salmeron-Sanchez, *Sci. Rep.* **2016**, *6*, 21809.
- [17] J. R. Van der Meer, J. Polman, M. M. Beerthuyzen, R. J. Siezen, O. P. Kuipers, W. M. De Vos, *J. Bacteriol.* **1993**, *175*, 2578.
- [18] M. Aumailley, M. Gurrath, G. Müller, J. Calvete, R. Timpl, H. Kessler, *FEBS Lett.* **1991**, *291*, 50.
- [19] K. Miyazono, Y. Kamiya, M. Morikawa, *J. Biochem.* **2010**, *147*, 35.
- [20] V. Llopis-Hernandez, M. Cantini, C. Gonzalez-Garcia, Z. A. Cheng, J. Yang, P. M. Tsimbouri, A. J. Garcia, M. J. Dalby, M. Salmeron-Sanchez, *Sci. Adv.* **2016**, *2*, e1600188.
- [21] A. Saadeddin, A. Rodrigo-Navarro, V. Monedero, P. Rico, D. Moratal, M. L. Gonzalez-Martin, D. Navarro, A. J. Garcia, M. Salmeron-Sanchez, *Adv. Healthcare Mater.* **2013**, *2*, 1213.
- [22] D. Zhu, F. Liu, H. Xu, Y. Bai, X. Zhang, P. E. J. Saris, M. Qiao, *FEMS Microbiol. Lett.* **2015**, *362*, fvn107; <https://doi.org/10.1093/femsle/fvn107>.
- [23] R. S. Bongers, M. H. N. Hoefnagel, M. J. C. Starrenburg, M. A. J. Siemerink, J. G. Arends, J. Hugenholtz, M. Kleerebezem, *J. Bacteriol.* **2003**, *185*, 4499.
- [24] O. P. Kuipers, P. G. G. A. De Ruyter, M. Kleerebezem, W. M. De Vos, *J. Biotechnol.* **1998**, *64*, 15.
- [25] P. Hols, M. Kleerebezem, A. N. Schanck, T. Ferain, J. Hugenholtz, J. Delcour, W. M. de Vos, *Nat. Biotechnol.* **1999**, *17*, 588.
- [26] S. Arioli, D. Zambelli, S. Guglielmetti, I. De Noni, M. B. Pedersen, P. D. Pedersen, F. Dal Bello, D. Mora, *Appl. Environ. Microbiol.* **2013**, *79*, 376.
- [27] G. S. Stein, J. B. Lian, *Endocr. Rev.* **1993**, *14*, 424.
- [28] A. Rodrigo-Navarro, P. Rico, A. Saadeddin, A. J. Garcia, M. Salmeron-Sanchez, *Sci. Rep.* **2014**, *4*, 5849.
- [29] J. J. Hay, A. Rodrigo-Navarro, K. Hassi, V. Moulisova, M. J. Dalby, M. Salmeron-Sanchez, *Sci. Rep.* **2016**, *6*, 21809.
- [30] J. Yang, L. E. McNamara, N. Gadegaard, E. V. Alakpa, K. V. Burgess, R. M. D. Meek, M. J. Dalby, *ACS Nano* **2014**, *8*, 9941.
- [31] H. Orimo, *J. Nippon Med. Sch.* **2010**, *77*, 4.
- [32] L. Malaval, F. Liu, P. Roche, J. E. Aubin, *J. Cell. Biochem.* **1999**, *74*, 616.
- [33] L. Steidler, J. M. Wells, A. Raeymaekers, J. Vandekerckhove, W. Fiers, E. Remaut, *Appl. Environ. Microbiol.* **1995**, *61*, 1627.
- [34] L. Schotte, L. Steidler, J. Vandekerckhove, E. Remaut, *Enzyme Microb. Technol.* **2000**, *27*, 761.
- [35] B. Benbouziane, P. Ribelles, C. Aubry, R. Martin, P. Kharrat, A. Riazi, P. Langella, L. G. Bermudez-Humaran, *J. Biotechnol.* **2013**, *168*, 120.
- [36] D. T. Riglar, P. A. Silver, *Nat. Rev. Microbiol.* **2018**, *16*, 214.
- [37] N. S. Forbes, *Nat. Rev. Cancer* **2010**, *10*, 785.
- [38] Z. Chen, L. Guo, Y. Zhang, R. L. Walzem, J. S. Pendergast, R. L. Printz, L. C. Morris, E. Matafonova, X. Stien, L. Kang, D. Coulon, O. P. McGuinness, K. D. Niswender, S. S. Davies, *J. Clin. Invest.* **2014**, *124*, 3391.
- [39] M. L. Hanson, J. A. Hixon, W. Li, B. K. Felber, M. R. Anver, C. A. Stewart, B. M. Janelins, S. K. Datta, W. Shen, M. H. McLean, S. K. Durum, *Gastroenterology* **2014**, *146*, 210.
- [40] A. D. Celiz, J. G. W. Smith, R. Langer, D. G. Anderson, D. A. Winkler, D. A. Barrett, M. C. Davies, L. E. Young, C. Denning, M. R. Alexander, *Nat. Mater.* **2014**, *13*, 570.
- [41] R. J. McMurray, N. Gadegaard, P. M. Tsimbouri, K. V. Burgess, L. E. McNamara, R. Tare, K. Murawski, E. Kingham, R. O. C. Oreffo, M. J. Dalby, *Nat. Mater.* **2011**, *10*, 637.
- [42] H. Shegarfi, O. Reikeras, *J. Orthop. Surg.* **2009**, *17*, 206.
- [43] S. C. Manolagas, *Endocr. Rev.* **2010**, *31*, 266.
- [44] R. J. Deans, A. B. Moseley, *Exp. Hematol.* **2000**, *28*, 875.
- [45] J. W. Sanders, G. Venema, J. Kok, *Appl. Environ. Microbiol.* **1997**, *63*, 4877.
- [46] D. Mu, M. Montalbán-López, Y. Masuda, O. P. Kuipers, *Appl. Environ. Microbiol.* **2013**, *79*, 4503.
- [47] F. P. Douillard, M. O'Connell-Motherway, C. Cambillau, D. van Sinderen, *Microb. Cell Fact.* **2011**, *10*, 66.